Notoginsenoside R1 alleviates spinal cord injury by inhibiting oxidative stress, neuronal apoptosis, and inflammation via activating the nuclear factor erythroid 2 related factor 2/heme oxygenase-1 signaling pathway

Hongbo Luo[a,*], Zhangli Bao[b,*], Mingjian Zhou[c], Yuxin Chen[a] and Zhaoxi Huang[d]

The secondary injury plays a vital role in the development of spinal cord injury (SCI), which is characterized by the occurrence of oxidative stress, neuronal apoptosis, and inflammatory response. Notoginsenoside R1 (NGR1) has been involved in the modulation of antioxidative stress and anti-inflammatory response. However, its roles in SCI-induced injury are still unknown. We explored the therapeutic effect of NGR1 and its underlying mechanism after SCI by using behavioral, biochemical, and immunohistochemical techniques. The administration of NGR1 after SCI enhanced the neurological function, and mitigated tissue damage and motor neuron loss than those in SCI + vehicle group. Meanwhile, significantly increased expression of Nrf2 protein and HO-1 protein was found in the SCI + NGR1 group compared with those in the SCI + vehicle group. In addition, the inhibitory effects of oxidative stress, apoptotic neuron ratio, and neuronal inflammation in the SCI + NGR1 group can be partially reversed when the Nrf2/HO-1 signaling pathway was inhibited by ML385. Our results indicate that the administration of NGR1 can attenuate oxidative stress, neuronal apoptosis, and inflammation by activating the Nrf2/HO-1 signaling pathway after SCI, thereby improving neurological function. *NeuroReport* 33: 451–462 Copyright © 2022 The Author(s). Published by Wolters Kluwer Health, Inc.

NeuroReport 2022, **33**:451–462

Keywords: apoptosis, notoginsenoside R1, Nrf2/HO-1 pathway, oxidative stress, spinal cord injury

Departments of [a]Rehabilitation, [b]Emergency, [c]Pediatrics and [d]Orthopedics, Ningde Municipal Hospital of Ningde Normal University, Ningde, China

Correspondence to Zhaoxi Huang, Department of Orthopedics, Ningde Municipal Hospital of Ningde Normal University, 7 North Road, Ningde, Fujian, 352100, China
E-mail: hzx05937636396@sina.com

*Hongbo Luo and Zhangli Bao contributed equally to the writing of this article.

Received 29 March 2022 **Accepted** 11 May 2022

Introduction

As a severe neurological disease, spinal cord injury (SCI) plays a crucial role in causing death and permanent disability in countries worldwide [1]. Most injuries of the spinal cord are comprised of the primary injury characterized by tissue damage and the secondary injury represented by progressive cell loss and death in the later stage [2]. The secondary injury of SCI will trigger the excessive accumulation of reactive oxygen species, which will further result in a series of complex biochemical changes, including edema, oxidative stress, initiation of neuronal apoptosis, and inflammation-dependent signaling pathways [3,4]. These changes trigger the physical and functional impairment following SCI and further exacerbate the continuous insult to the tissues around the epicenter of the injury site [5,6]. Therefore, it is imperative to further illustrate the potential mechanisms of secondary damage and explore effective therapeutic strategies to inhibit oxidative stress, neuronal apoptosis, and inflammatory response caused by secondary damage.

Notoginsenoside R1 (NGR1), namely $C_{47}H_{80}O_{18}$, is the major active component extracted from the traditional Chinese medicine called Panax notoginseng [7]. It is closely related to the antioxidative stress, anti-inflammatory response, antiangiogenesis, and antiapoptotic effects [8–10]. It has been reported that NGR1 can exert anti-inflammatory and antiapoptotic activities through the phosphatidylinositol-3-kinase/protein kinase B (PI3K/AKT) axis, thereby reducing cardiac dysfunction and improving renal dysfunction caused by ischemia/reperfusion [11,12]. What is more, NGR1 treatment improves cognitive function and enhancing the expression of insulin degrading enzyme in an Alzheimer's disease mouse model [13]. In addition, recent study has proved that NGR1 administration protects PC-12 cells against LPS-induced inflammatory insult through upregulating the expression of miR-132 [14]. However, the therapeutic effect and underlying mechanism of NGR1 on traumatic SCI have not been thoroughly investigated.

The basic leucine zipper transcription molecule nuclear factor erythroid 2 related factor 2 (Nrf2) with Cap'n' collar structure is widely expressed in various tissues [15]. Recently, accumulating evidences have shown its crucial role in maintaining the balance of endogenous redox state and the expression of genes related to cell metabolism,

0959-4965 Copyright © 2022 The Author(s). Published by Wolters Kluwer Health, Inc. DOI: 10.1097/WNR.0000000000001803

cell protection, immune response, and cell cycle homeostasis [16–18]. As a transcription factor of stress response, Nrf2 exerts a neuroprotective role in various nervous system diseases including traumatic SCI [19]. In addition, Nrf2 has also been shown to participate in controlling the expression of antioxidant response element-driven genes, which encode antioxidant/detox enzymes such as Heme oxygenase-1 (HO-1) [20]. Endogenous HO-1 is shown to exist in spinal cord neurons following SCI insult and HO-1 overexpression promotes functional recovery and prohibits the formation of NLRP1 inflammasome after SCI injury [21,22]. What is more, HO-1 treatment has also been shown to inhibit acute SCI-induced disruption of the blood-spinal cord barrier and the initiation of oxidative stress [23]. Therefore, we hypothesize that NGR1 treatment can attenuate SCI-induced neurological impairment by activating the Nrf2/HO-1 signaling pathway.

In this study, we established a rat SCI model to explore the therapeutic roles of NGR1 as well as its potential mechanisms for regulating oxidative stress, neuronal apoptosis, and inflammatory response. Our findings further clarify our knowledge of Nrf2 and provide more theoretical basis for future clinical treatment of SCI.

Materials and methods

Experimental animals

A total of 52 adult male Sprague–Dawley rats (weighed 280–300 g and aged 12–14 weeks old) were purchased from Shanghai SLAC Laboratory Animal Co. Ltd (Shanghai, China). The rats were kept in a humidity-controlled room (25 ± 1 °C, 60–70% humidity, and with lights between 7:00 a.m. and 7:00 p.m.) and were given free access to food and water. All rats were cared for in accordance with the National Institutes of Health guide for the care and use of Laboratory animals (NIH Publications No. 8023, revised 1978). All study procedures were approved by the Ningde Municipal Hospital Institutional Animal Care and Use Committee.

Spinal cord injury model

The experimental SCI model was established in rats by the modified weight-drop method as previously described [24]. Briefly, before SCI, rats were anesthetized with intraperitoneal injections of pentobarbital (50 mg/kg, b.w.) and then fixed on the operating table in the prone position. There is no rat exhibited signs of peritonitis, pain or discomfort following administration of 10% chloral hydrate. A 3-cm midline incision was made at the level of the T12 vertebra to fully expose the vertebrae and perform laminectomy using tissue scissors. Then, a 10 g impactor device with a diameter of 2 mm was dropped freely at a height of 2.5 cm to completely impact the spinal cord, then it was immediately removed to form an injury area of a specific size. After being impacted, the rats will have tail sway reflex and twitching and contraction of both hind limbs and body, which is the stress reflex of the rats, and indicates that the SCI model was successfully performed. The rats in the sham operation group underwent the same surgical procedure as the SCI group, except that they did not suffer spinal cord impact. After the operation, the urinary bladder of the rats (excluding those in the sham group) underwent manually emptying twice a day to assist in urinating until the rats were able to urinate normally.

Experimental groups and drug treatments

Rats were randomly divided into the following five groups and drug administration was performed by an investigator who was blind to the drugs. NGR1 (MedChemExpress, Shanghai, China, Cat# HY-N0615) was freshly dissolved in the vehicle [dimethylsulfoxide (DMSO) and 0.9% NaCl, 1:3] and given at a dose of 25 mg/kg. ML385 (Nrf2 inhibitor) (MedChemExpress, Shanghai, China, Cat# HY-100523) was freshly dissolved in the vehicle (DMSO and 0.9% NaCl, 1:3) and given at a dose of 30 mg/kg. The administration dose of NGR1 and ML385 was selected according to that previously described [11,25].

(1). Sham + vehicle group: rats were treated with the same amount of vehicle (DMSO and 0.9% NaCl, 1:3) by intraperitoneal injection (i.p.) every day for a total of 21 days (n = 30).
(2). Sham + NGR1 group: rats were treated with NGR1 (25 mg/kg/day, i.p.) for a total of 21 days (n = 30).
(3). SCI + vehicle group: the rats were administrated with the same amount of vehicle (DMSO and 0.9% NaCl, 1:3, i.p.) every day for a total of 21 days 2 h after SCI (n = 30).
(4). SCI + NGR1 group: the rats were administrated with NGR1 (25 mg/kg/day, i.p.) for a total of 21 days 2 h after SCI (n = 30).
(5). SCI + NGR1 + ML385 group: after contusion, the rats were immediately injected with NGR1 (25 mg/kg/day, i.p.) and ML385 (30 mg/kg/day, i.p.) for a total of 21 days 2 h after SCI (n = 30).

Locomotion recovery assessment

The recovery of behavioral function was assessed using the Basso-Beattie-Bresnahan (BBB) Locomotor Scale at 1, 3, 7, 14, and 21 days following surgery procedures as previously described [26]. Briefly, rats were placed individually in an open field and observed for 4 min by two observers who were blind to the experiment. The scores of rats from each group (n = 6) were recorded, and the data used for analysis were represented as mean scores. BBB scores were graded on a scale of 0–21 (0: complete paralysis and 21: normal locomotion).

Tissue preparation

Rats were anesthetized with intraperitoneal injections of 10% chloral hydrate (300 mg/kg, b.w.) on day 21 after SCI. An incision was made at the midline of the sternum to expose the heart, and 0.9% precooled saline was slowly perfused transcranially. About 1 cm of spinal cord

tissue samples surrounding the damaged region was obtained on ice. For biochemical analysis, the samples were immediately transferred to liquid nitrogen and stored at a refrigerated temperature of about –80 °C. For histopathological analysis, the samples were fixed in 4% paraformaldehyde at 4 °C overnight and then dehydrated in a 30% sucrose solution and a 20% sucrose solution in turn. The thickness of 10-μm spinal cord sections was cut using a cryostat at –20 °C for further analysis.

Hematoxylin-eosin staining and Nissl staining

The spinal cord tissue sections were used for hematoxylin-eosin (HE) staining using HE solution according to the manufacturer's instructions 21 days after SCI. Briefly, after being stained with hematoxylin for 30 s, 10-μm tissue sections were quickly washed in deionized water. Then, these sections were further differentiated in the 0.5% HCl solution (dissolved in 95% alcohol) for 6 s. After being washed in deionized water for 1 h, the sections were continuously stained with eosin and, subsequently, were fixed with neutral gum after dehydration using a series of ethanol. Then, these slides were observed under a microscope and the Image J software was used for analyzing the proportion of preserved tissue as previously described [27].

Nissl staining was conducted according to the manufacturer's instructions 21 days after SCI. Briefly, the spinal cord sections were dried at room temperature for 2 h and then incubated in the ethanol/chloroform mixed solution overnight. The next day, the sections were soaked in 100% ethanol, 75% ethanol, and distilled water for 1 min, and then incubated in 37% 0.1% cresol purple solution for 5 min. Then, the sections were immersed in anhydrous ethanol and xylene for another 5 min. After being sealed with neutral gum, these slides then were observed under a microscope and the Image J software was used for analyzing the average number of survival neurons of three different visual fields on each slide. Five sections per animal were processed for Nissl staining.

Western blot analysis

The spinal cord tissues obtained 21 days after SCI were homogenized and lysed in radio immunoprecipitation assay (RIPA) buffer (Beyotime Biotechnology, China) containing phenylmethanesulfonyl fluoride, protease, and phosphatase inhibitor cocktails (Beyotime Biotechnology, China) for 30 min on ice. The supernatants of tissue lysates were collected after being centrifuged at 12 000 rpm for 30 min at 4 °C, and then, the protein concentration was quantified using the BCA Protein Assay Kit (Thermo, Massachusetts, USA). A total of 40-μg protein was separated using SDS-PAGE and transferred onto polyvin ylidene difluoride (PVDF) membranes. The membranes were blocked with 5% skimmed milk in triethanolamine buffered saline-Tween (TBST) for 1.5 h at room temperature. After washing, these PVDF membranes were incubated at 4 °C overnight with the following primary antibodies: anti-Nrf2 (1:1000, Abcam, Massachusetts, USA, Cat# ab137550), anti-Heme Oxygenase-1 (1:2000, Abcam, Massachusetts, USA, Cat# ab189491), anti-NAD(P)H quinone oxidoreductase 1 (anti-NQO1) (1:1000, Abcam, Massachusetts, USA, Cat# ab80588), anti-Cleaved Caspase-3 (1:1000, Proteintech, Wuhan, China, Cat#19677-1-AP), anti-Caspase-9 (1:500, Proteintech, Wuhan, China, Cat# 10380-1-AP), anti-Bcl-2 (1:1000, Abcam, Cambridge, Massachusetts, USA, Cat# ab32124), anti-Bax (1:1000, Abcam, USA, Cat# ab250635), anti-IL-6 (1:500, Abclonal, Wuhan, China, Cat# A0286), anti-IL-1β (1:1000, Abclonal, Wuhan, China, Cat# A1112), anti-TNFα (1:1500, Abclonal, Wuhan, China, Cat# A11534) and anti-β-actin (1:400, Boster, Wuhan, China, Cat# BM3873). The next day, the membranes were washed with TBST for three times and then incubated with the following secondary antibodies (goat anti-rabbit, 1:10000, Abcam, Cambridge, Massachusetts, USA, Cat# ab6721; goat anti-mouse, 1:10000, Abcam, Cambridge, Massachusetts, USA, Cat# ab6789) at room temperature for 1.5 h. The immunoreactive bands were visualized using an imaging system (Bio-Rad, California, USA) and the Image J software was used for measuring band intensity.

Real-time-PCR analysis

The total RNA from the spinal cord tissues obtained was extracted using Trizol reagent (Invitrogen, California, USA) 21 days after SCI according to the manufacturer's instructions. Briefly, cDNA was generated from total RNA (1 μg) using the TaKaRa RNA PCR kit (AMV) Ver. 3.0 (Takara, Japan). The mRNA expressions of IL-6, IL-1β, TNF-α, and β-actin were examined using cDNA as a template by the following primers: IL-6 (forward primer 5′- ATACCACCCACAACAGACCAGT-3′ and reverse primer 5′-GATGAGTTGGATGGTCTTGGT -3′); IL-1β (forward primer 5′- CTCTGTGACTC GTCGTGG GATGATG -3′ and reverse primer 5′- CACTTGTTGGCTTATGTTCTGTCC -3′); TNF-α (forward primer 5′- CCCAGACCCTCA CACTCAGATCAT -3′ and reverse primer 5′- CAGCCTTGTCCCTTGA AGAGAA -3′; β-actin (forward primer 5′-ATATCGCTGCGCTCGTCG-3′ and reverse primer 5′-CAATGCCGTGTTCAATGGGG-3′). The amplification was done for 27 cycles at 92 °C for 30 s, 50 °C for 30 s and 70 °C for 1 min. Final extension was performed at 70 °C for 10 min. The expression of relative mRNA was calculated using the $2^{-\Delta\Delta Ct}$ method.

Immunofluorescence analysis

The sections from the spinal cord tissues acquired 21 days after SCI were used for immunofluorescence staining as previously described with minor modifications. Briefly, the 10-μm sections were dried for 1 h at room temperature and incubated with blocking solution (5% goat serum in phosphate buffered solution-tween 20) for 2 h at room temperature. Then, the sections were incubated at 4 °C overnight

with the following primary antibodies: anti-NeuN antibody (1:300, Abcam, USA) and anti-Nrf2 (1:100, Abcam, USA). The next day, after being washed three times with phosphate buffered solution, the sections were incubated with the following secondary antibodies (488 goat anti-rat IgG, 1:500, Invitrogen, California, USA, and 594 goat anti-mouse, 1:500, Invitrogen, California, USA) for 2 h at room temperature. The sections were then incubated with DAPI for 15 min and sealed with a coverslip. The images were visualized using a fluorescent microscopy (Olympus, Tokyo, Japan). The Image J software was used for analyzing the overlap coefficient of HO-1 with neurons.

TUNEL staining analysis

The sections were used for TUNEL staining 21 days after SCI using an In Situ Cell Death Detection kit (Roche, Germany, Cat# 11684795910) according to the manufacturer's instructions. Briefly, rewarmed sections were fixed in 4% paraformaldehyde and incubated with 2% H_2O_2. After being washed three times, the sections were incubated with reaction mixture solution for 2 h at 37 °C and then blocked with 2% BSA for 1 h. Finally, the sections were counterstained with hematoxylin. The images were visualized using a fluorescent microscopy (Olympus, Tokyo, Japan) and the Image J software was used for counting TUNEL-positive cells. Data were presented as a mean percentage of the number of TUNEL-positive cells in the whole fields of view from six randomly selected fields in each per experiment.

Measurement of antioxidants and oxidative products

The spinal cord tissues obtained 21 days after SCI were lysed with RIPA buff, and the levels of spinal malonaldehyde (MDA), superoxide dismutase (SOD), and glutathione peroxidase activity (GSH-PX) were measured by the MDA assay Kit (NanJing JianCheng Bioengineering Institute, Nanjing, China, Cat# A003-4-1), the SOD assay Kit (NanJing JianCheng Bioengineering Institute, Nanjing, China, Cat# A001-3-2), and the GSH-PX assay Kit (NanJing JianCheng Bioengineering Institute, Nanjing, China, Cat# A005-1-2) according to the manufacturer's instructions.

Statistical analysis

Data were presented as mean ± SEM and processed by SPSS 22.0. statistical software. Comparisons among multiple groups were performed by one-way analysis of variance (ANOVA), followed by Turkey's post hoc tests. The significance of the BBB scores was analyzed by two-way repeated-measures ANOVA), followed by Bonferroni post hoc test. *P*-values <0.05 were considered statistically significant.

Results

Notoginsenoside R1 improves the neurological function after spinal cord injury

To evaluate the roles of NGR1 in improving SCI, we first examined the BBB scores at 1, 3, 7, 14, and 21 days after SCI. Normal scores (21 points) were observed in the Sham + vehicle group and Sham + NGR1 group. The BBB scores in the SCI + vehicle group were declined and the same as those in the SCI + NGR1 group at 1 day after SCI. What is more, the BBB scores in the SCI + NGR1 group were higher than those in the SCI + vehicle group but no significant difference was found between the two groups at 3 and 7 days after SCI. However, the BBB scores were markedly elevated in rats administrated with NGR1 than those in the SCI + vehicle group at 14 days following SCI. Furthermore, a more remarkable difference between the SCI + vehicle group and SCI + NGR1 group was found at 21 days following SCI. This result indicated that NGR1 treatment may have a potential therapeutic effect on neurological function following SCI (Fig. 1).

Notoginsenoside R1 alleviates tissues damage and motor neurons loss after spinal cord injury

To further explore the neuroprotective effects of NGR1 treatment on SCI, we perform the HE staining to examine the histopathological changes of rats and Nissl staining to observe the loss of motor neurons 21 days following SCI. HE staining showed that the Sham + vehicle group and the Sham + NGR1 group presented normal structure of spinal cord tissues. However, the structural damage was obvious in the SCI + vehicle group characterized by a larger cavity. NGR1 treatment exhibited a smaller cavity and a larger ratio of intact neuron tissues than that in the SCI + vehicle group (Fig. 2a and b). Nissl staining demonstrated that the spinal anterior horn of rats suffered

Fig. 1

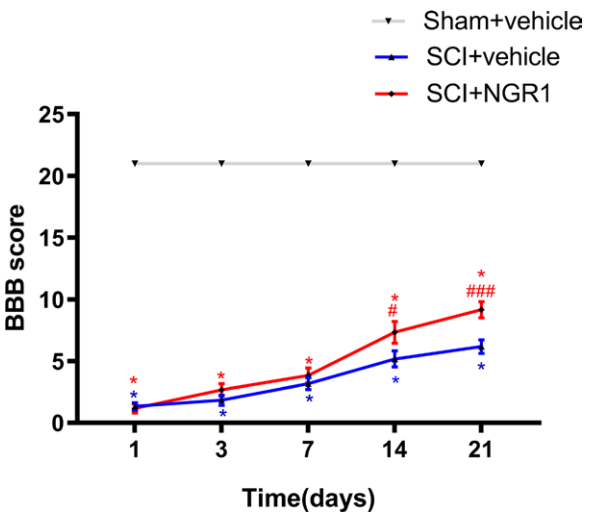

NGR1 administration improves neurological function after SCI. BBB scores of the Sham + vehicle, Sham + NGR1, SCI + vehicle, and SCI+NGR1 groups were examined at 1, 3, 7, 14, and 21 days after SCI. $N = 6$. Data are represented as mean ± SEM. Repeated-measures analysis of variance (ANOVA) followed by Bonferroni's multiple comparisons posttest was used. $^{*}P < 0.05$ vs. the Sham + vehicle group; $^{\#}P < 0.01$, $^{\#\#\#}P < 0.001$ vs. the SCI + vehicle group. BBB, Basso-Beattie-Bresnahan; NGR1, notoginsenoside R1; SCI, spinal cord injury.

Fig. 2

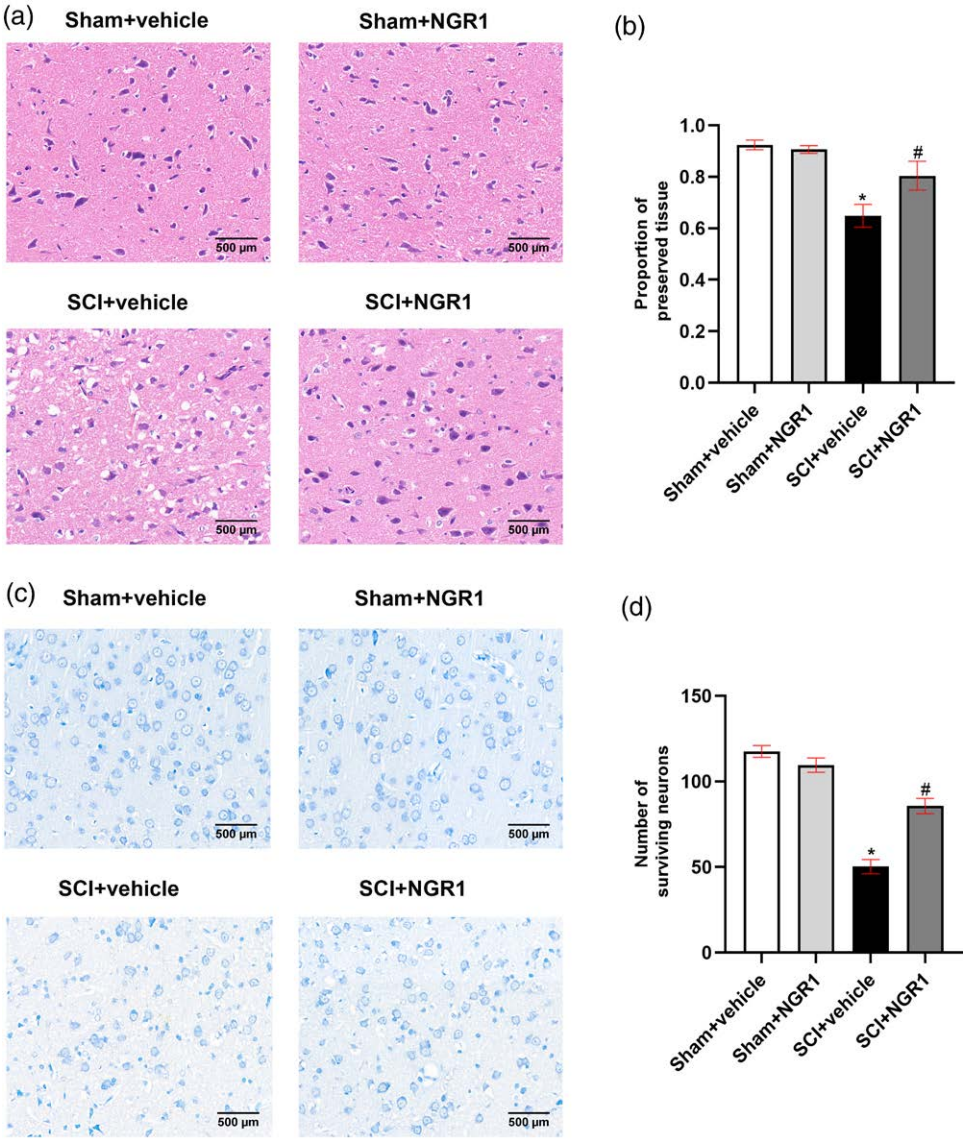

NGR1 administration attenuates tissue damage and motor neurons loss after SCI. (a) The representative image of HE staining in the Sham + vehicle, Sham + NGR1, SCI + vehicle, and SCI+NGR1 groups at 21 days after SCI. Bars = 500 μm (200×). (b) Quantitative analysis of the proportion of preserved tissue in each group. $N = 6$. Data are represented as mean ± SEM. $^*P < 0.05$ vs. the Sham + vehicle group; $\#P < 0.05$ vs. the SCI+NGR1 group. (c) The representative image of Nissl staining in the Sham + vehicle, Sham + NGR1, SCI + vehicle, and SCI + NGR1 groups at 14 days after SCI. Bars = 500 μm (200×). (d) Quantitative analysis of the number of surviving neurons in each group. $N = 6$. Data are represented as mean ± SEM. One-way analysis of ANOVA with Turkey's post hoc tests was used. $^*P < 0.05$ vs. the Sham + vehicle group; $\#P < 0.05$ vs. the SCI+NGR1 group. ANOVA, analysis of variance; HE, hematoxylin-eosin; NGR1, notoginsenoside R1; SCI, spinal cord injury.

a great loss of motor neurons following SCI and the SCI + NGR1 group presented a similar result. However, motor neurons in the SCI + NGR1 group were markedly preserved and the number of survival motor neurons were significantly higher than those in the SCI + vehicle group. These results showed that NGR1 treatment may play a crucial role in decreasing the damage of spinal cord tissues and motor neuron loss in SCI rats.

Notoginsenoside R1 activates Nrf2/HO-1 signaling pathway after spinal cord injury

In order to evaluate the potential mechanism of NGR1 exerting neuroprotective effects after SCI, we performed western blot and immunofluorescence to analyze the expression of Nrf2, HO-1, and NQO1 protein in spinal cord tissues 21 days after SCI. The SCI + vehicle group exhibited slightly higher protein levels of Nrf2 and HO-1 than those in the Sham + vehicle group,

whereas an obvious decline in NQO1 protein level was found in the SCI + vehicle group. What is more, compared with SCI + vehicle group, NGR1 administration markedly elevated the expression of Nrf2 and HO-1 protein and these increases could be partly inhibited in the SCI + NGR1 + ML385 (Nrf specific inhibitor) group. However, no significant difference in NQO1 protein level was detected in the SCI + vehicle group, the SCI + NGR1 group, and the SCI + NGR1 + ML385 group (Fig. 3a–d). Immunofluorescence staining demonstrated that rats underwent SCI presented slightly higher HO-1 protein level, and NGR1 treatment further increased the HO-1 protein level, whereas this activation effect was inhibited when combined application of NGR1 and ML385 (Fig. 3e–f). These results indicated that NGR1 administration may participate in the activation of Nrf2/HO-1 signaling pathway following SCI.

Notoginsenoside R1 inhibits oxidative stress through Nrf2/HO-1 signaling pathway after spinal cord injury

To examine the role of NGR1 treatment in oxidative stress after SCI, we detected the activities of MDA, SOD, and GSH-PX in spinal cord tissues 21 days after SCI. A significant increase of MDA level and a marked reduction of SOD and GSH-PX activities were observed in the SCI + vehicle group than those in Sham + vehicle group. Compared with the SCI + vehicle group, NGR1 administration curtailed the expression of MDA level and enhanced the activities of SOD and GSH-PX. Compared with the SCI + NGR1 group, the combined application of NGR1 and ML385 after SCI partly reinforced the MDA level and inhibited the SOD and GSH-PX activities (Fig. 4a–c). These results indicate that NGR1 administration may inhibit oxidative stress by activating the Nrf2/HO-1 signaling pathway to improve neurological function after SCI.

Notoginsenoside R1 attenuates neuronal apoptosis through Nrf2/HO-1 signaling pathway after spinal cord injury

To evaluate the effect of NGR1 treatment on neuronal apoptosis after SCI, we first performed Western Blot to detect the expression levels of antiapoptotic protein Bcl-2 and proapoptotic protein Caspase-9, Caspase-3, and Bax 21 days after SCI. Compared with the Sham + vehicle group, the expression of Bcl-2 protein decreased accompanied by the enhancement of Cleaved caspase-9, Cleaved caspase-3, and Bax protein levels. However, NGR1 administration markedly reinforced the expression of Bcl-2 protein and curtailed the expression of Cleaved caspase-9, Cleaved caspase-3, and Bax protein levels than those in the Sham + vehicle group. What is more, compared with the SCI + NGR1 group, the combined application of NGR1 and ML385 partly inhibited the enhancement of Bcl-2 protein level and the reduction of Cleaved caspase-9, Cleaved caspase-3, and Bax protein levels (Fig. 5a–e). In addition, TUNEL staining was also conducted to analyze the apoptotic neurons. The percentage of TUNEL-positive cells in the SCI + vehicle group was markedly higher than that in the Sham + vehicle group. While compared with the SCI + vehicle group, NGR1 treatment significantly downregulated the expression of TUNEL-positive cells. NGR1 combined with ML385 treatment after SCI could partly enhance the percentage of TUNEL-positive cells than that in the SCI + NGR1 group (Fig. 5f and g). These results indicated that NGR1 administration may exert an antiapoptotic effect by activating Nrf2/HO-1 signaling pathway after SCI.

Notoginsenoside R1 inhibits neuronal Inflammation through Nrf2/HO-1 signaling pathway after spinal cord injury

To verify the role of NGR1 treatment in neuronal Inflammation after SCI, we detected the mRNA and protein expression of downstream inflammatory cytokines 21 days after SCI. The mRNA and protein levels of IL-6, IL-1β, and TNF-α were appreciably raised in SCI rats than those in the Sham + vehicle group, whereas these increases were hindered by the application of NGR1 after SCI. In addition, these reductions of downstream inflammatory cytokines in the SCI + NGR1 group could be partly blocked when combining NGR1 with ML385 treatment in the rats subjected to SCI (Fig. 6a–g). These results indicated that NGR1 administration may downregulate the activities of inflammatory cytokines through activating Nrf2/HO-1 signaling pathway to exert neuroprotective effects after SCI.

Discussion

In this study, we explored the neuroprotective effect of NGR1 in SCI rats and its potential mechanism. We found that NGR1 administration reduced oxidative stress, neuronal apoptosis, and neuronal inflammation via activating the Nrf2/HO-1 signaling pathway in rats subjected to SCI, thereby improving neural functional recovery and inhibiting tissues damage and motor neurons loss.

SCI is a serious and unpredictable complication that causes limb dysfunction and permanent disability worldwide [28]. During the occurrence and development of SCI disease, secondary injury is the main stage leading to spinal cord dysfunction, and is a complex process regulated by a series of pathological mechanisms (such as edema, neuronal inflammation, and oxidative stress) [29]. However, the specific molecular mechanism of the secondary injury has not been thoroughly investigated. Therefore, in this study, we further explored the pathology mechanisms of the secondary injury stage and effective therapeutic strategies to block the secondary injury after SCI.

As an important phytoestrogen, the role of NGR1 in a variety of disease models has been extensively investigated.

Fig. 3

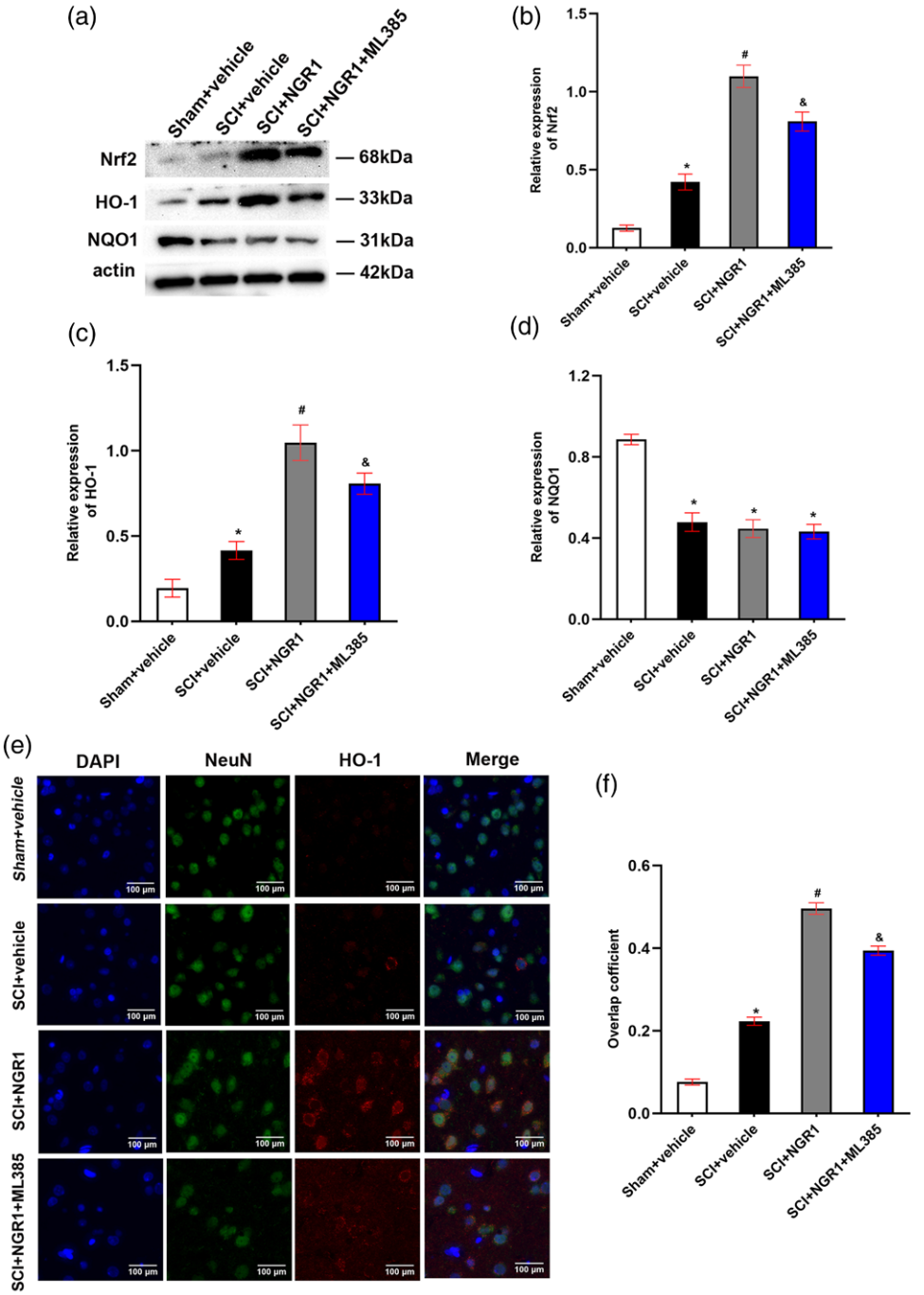

NGR1 administration activates Nrf2/HO-1 signaling pathway after SCI. (a) The representative image of Western Blot analysis for Nrf2, HO-1, and NQO1 in the Sham + vehicle, SCI + vehicle, SCI + NGR1, and SCI+NGR1+ML385 groups at 21 days after SCI. (b–d) Quantitative analysis of Nrf2/actin, HO-1/actin, and NQO1/actin in each group. $N = 3$. Data are represented as mean ± SEM. One-way analysis of ANOVA with Turkey's post hoc tests was used. $^{*}P < 0.05$ vs. the Sham + vehicle group; $^{\#}P < 0.05$ vs. the SCI + vehicle group; $^{\&}P < 0.05$ vs. the SCI + NGR1 group. (e) The representative image of immunofluorescence analysis for HO-1 in the Sham + vehicle, SCI + vehicle, SCI + NGR1, and SCI + NGR1 + ML385 groups at 3 days after SCI. Bars = 100 μm (400×). (f) Quantitative analysis of the overlap coefficient in each group. $N = 3$. Data are represented as mean ± SEM. $^{*}P < 0.05$ vs. the Sham + vehicle group; $^{\#}P < 0.05$ vs. the SCI + NGR1 group. ANOVA, analysis of variance; HO-1, heme oxygenase-1; NGR1, notoginsenoside R1; Nrf2, nuclear factor erythroid 2 related factor 2; NQO1, anti-NAD(P)H quinone oxidoreductase 1; SCI, spinal cord injury.

Fig. 4

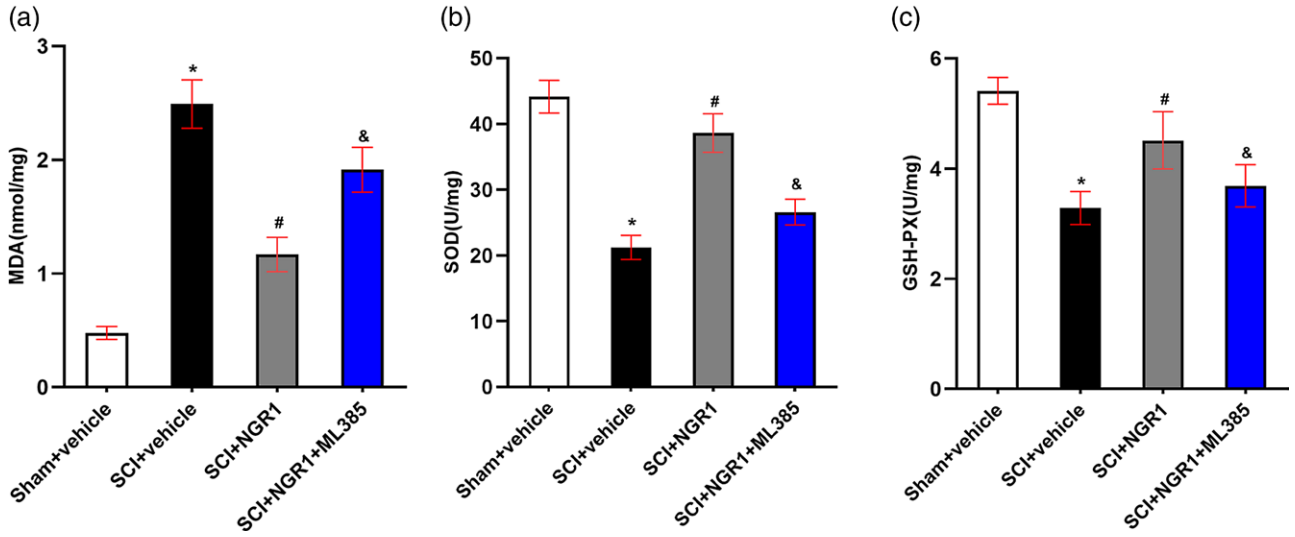

Involvement of the Nrf2/HO-1 signaling pathway in the NGR1-induced inhibition of oxidative stress after SCI. (a–c) Quantitative analysis of MDA, SOD, GSH-PX in the Sham + vehicle, SCI + vehicle, SCI + NGR1, and SCI + NGR1 + ML385 groups at 14 days after SCI. $N = 5$. Data are represented as mean ± SEM. One-way analysis of ANOVA with Turkey's post hoc tests was used. $^{*}P < 0.05$ vs. the Sham + vehicle group; $^{\#}P < 0.05$ vs. the SCI + vehicle group; $^{\&}P < 0.05$ vs. the SCI + NGR1 group. ANOVA, analysis of variance; GSH-PX, glutathione peroxidase activity; HO-1, heme oxygenase-1; MDA, malonaldehyde; NGR1, notoginsenoside R1; Nrf2, nuclear factor erythroid 2 related factor 2; SCI, spinal cord injury; SOD, superoxide dismutase.

For example, NGR1 administration protects against different organs ischemia/reperfusion injury such as heart, kidney, intestinal, and brain through attenuating oxidative stress, cell apoptosis, inflammatory response, and improving the ability of energy metabolism [30]. What is more, the treatment of NGR1 improves diabetic retinopathy-induced retinal dysfunction and elevates the level of mitophagy via PINK1/Parkin signaling pathway [31]. In addition, the cardioprotective effects of NGR1 pretreatment were also observed in rats with diabetic cardiomyopathy [32]. Previous study also demonstrates that the administration of NGR1 attenuates lipopolysaccharide-induced inflammatory response by stimulating the expression of miR-132 in PC-12 cell [14]. In recent years, the diversity effect of NGR1 in adult animals has aroused increasing research interest. We, therefore, performed this experiment to explore the neuroprotective roles and the potential molecular mechanisms of NGR1 administration in the in-vivo SCI model.

Nrf2, a sensor regulating the balance between the antioxidant system and the oxidant system, can be activated under various stressful conditions. As a downstream gene of Nrf2, HO-1 can also maintain the cellular function by binding to Nrf2. Previous studies have found that Nrf2/HO-1 axis is involved in cytoprotective effects in a variety of diseases, including cardiovascular diseases, neurodegenerative diseases, and SCI [33–35]. However, another study demonstrates that Nrf2 pathway also plays a vital role in the occurrence and progression of a variety of diseases [36]. These discrepant results indicate that Nrf2 pathway may have a dual effect in pathology conditions. Previous study proves that an elevated Nrf2 protein level is found 30 min after SCI and persists for 3 days, accompanied by the enhancement of the HO-1 protein level ranged from 1 to 3 days post-SCI, whereas no significant changes in NQO1 were observed 3 days after SCI [37]. In our current study, the expression of Nrf2 and HO-1 protein increased, whereas the expression of NQO1 protein decreased significantly. This inconsistent result may be due to the differences in rats' sex, tissue extraction sites, and observation time. What is more, NGR1 treatment could promote the expression of Nrf2 and HO-1 but not NQO1 protein levels, whereas the Nrf2 inhibitor ML385 partly blocked the increase of Nrf2 and HO-1 protein levels, which was consistent with previous study demonstrating that Nrf2 and HO-1 can be activated in mice with diabetic nephropathy treated with NGR1 [32]. Thus, these findings showed that the neuroprotective effect of NGR1 may be associated with the Nrf2/HO-1 signaling pathway.

The initiation of oxidative stress and neuronal apoptosis is the major pathology feature during the progression of secondary injury following SCI [38]. SCI results in the imbalance between the oxidant and antioxidant systems, which is represented by the reduction of antioxidant enzymes and the accumulation of oxidant molecules [39]. In addition, oxidative injury further causes excessive activation of proapoptotic factors and inhibition

Fig. 5

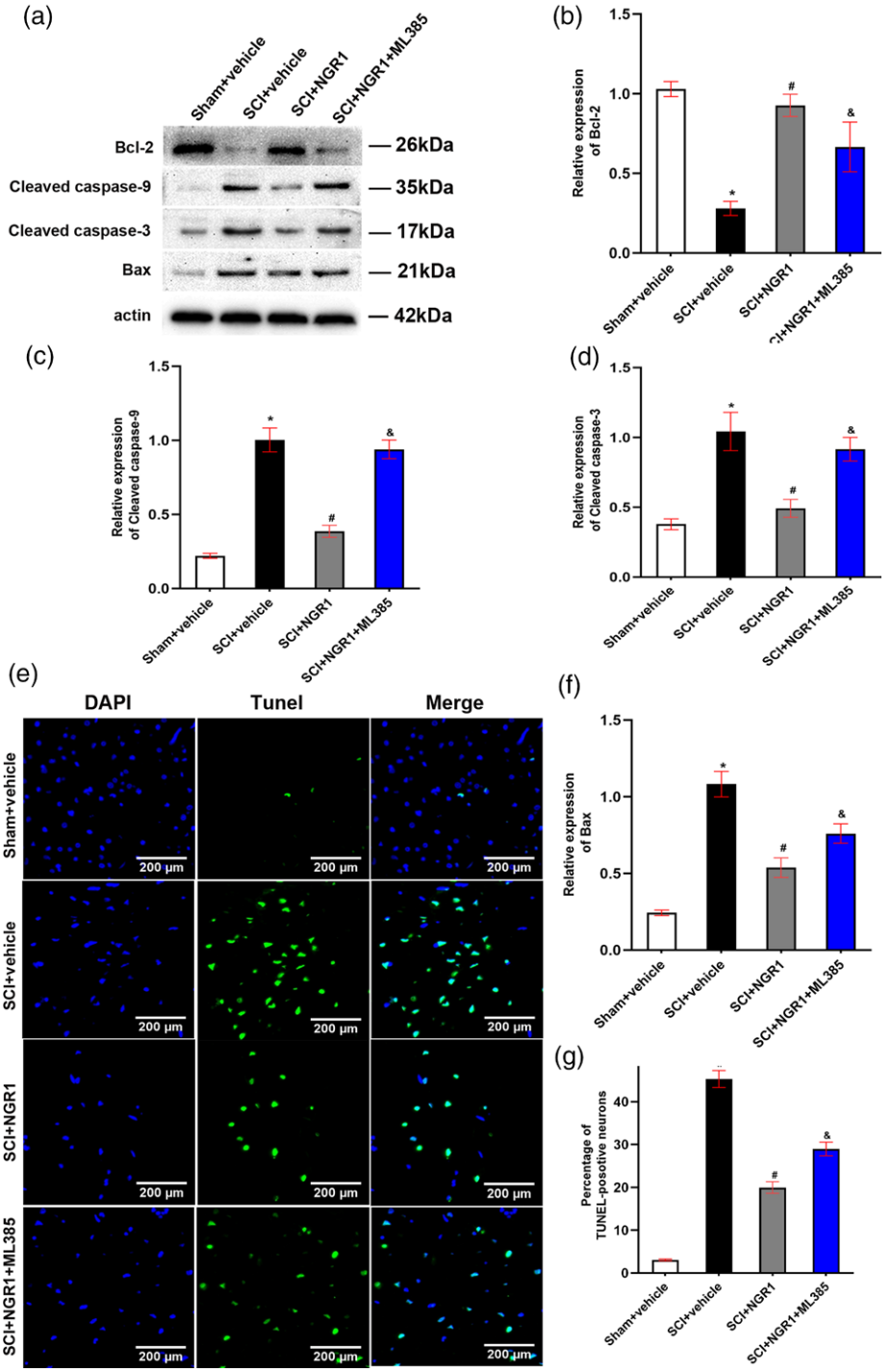

Involvement of the Nrf2/HO-1 signaling pathway in the NGR1-induced inhibition of apoptosis after SCI. (a) The representative image of Western Blot analysis for Bcl-2, c-Caspase-9, c-Caspase-3, and Bax in the Sham + vehicle, SCI + vehicle, SCI + NGR1, and SCI + NGR1 + ML385 groups at 14 days after SCI. (b–e) Quantitative analysis of Bcl-2/actin, Cleaved caspase-9/actin, Cleaved caspase-3/actin and Bax/actin in each group. $N = 3$. Data are represented as mean ± SEM. $^{*}P < 0.05$ vs. the Sham + vehicle group; $^{\#}P < 0.05$ vs. the SCI + vehicle group; $^{\&}P < 0.05$ vs. the SCI + NGR1 group. (f) The representative image of Tunel staining in the Sham + vehicle, SCI + vehicle, SCI + NGR1, and SCI + NGR1 + ML385 groups at 14 days after SCI. Bars = 200 μm (200×). (g) Quantitative analysis of the percentage of TUNEL-positive neurons in each group. $N = 3$. Data are represented as mean ± SEM. One-way analysis of ANOVA with Turkey's post hoc tests was used. $^{*}P < 0.05$ vs. the Sham + vehicle group; $^{\#}P < 0.05$ vs. the SCI + NGR1 group; $^{\&}P < 0.05$ vs. the SCI + NGR1 group. ANOVA, analysis of variance; HO-1, heme oxygenase-1; NGR1, notoginsenoside R1; Nrf2, nuclear factor erythroid 2 related factor 2; SCI, spinal cord injury.

Fig. 6

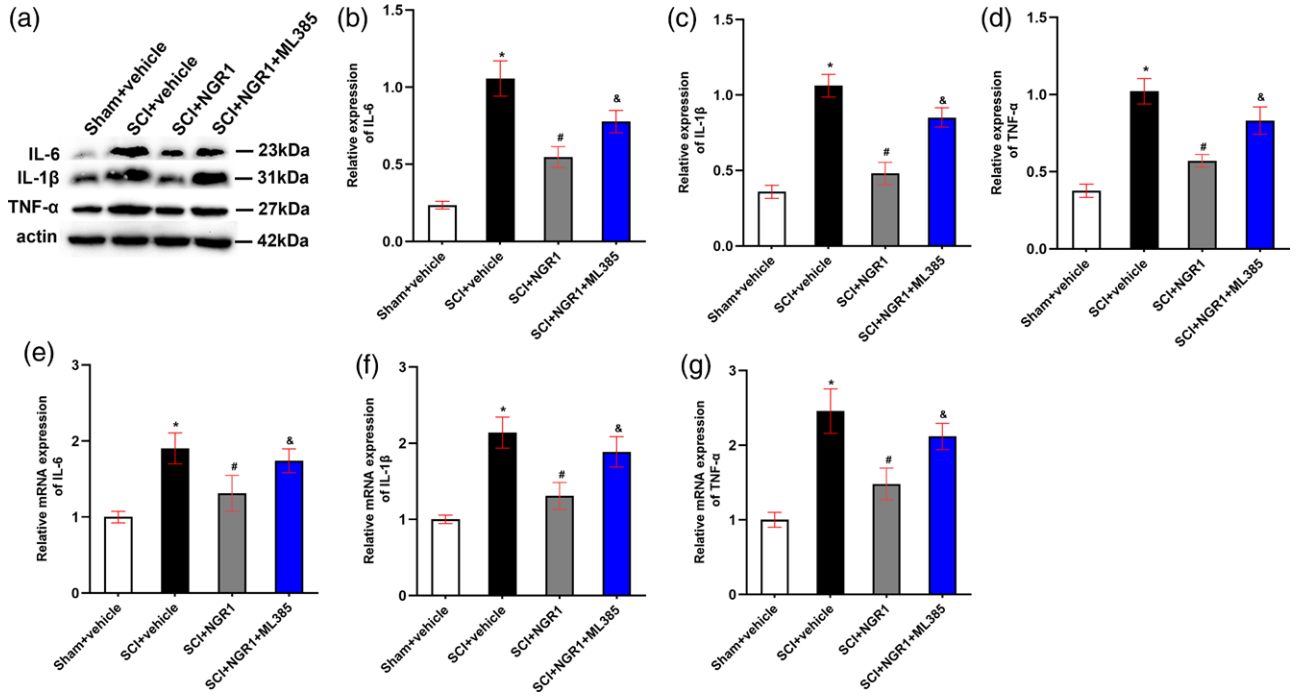

Involvement of the Nrf2/HO-1 signaling pathway in the NGR1-induced attenuation of neuronal inflammation after SCI. (a) The representative image of Western Blot analysis for IL-6, IL-1β, and TNF-α in the Sham + vehicle, SCI + vehicle, SCI + NGR1, and SCI + NGR1 + ML385 groups at 21 days after SCI. (b–d) Quantitative analysis of IL-6/actin, IL-1β/actin, and TNF-α/actin in each group. $N = 3$. Data are represented as mean ± SEM. $^{*}P < 0.05$ vs. the Sham + vehicle group; $^{\#}P < 0.05$ vs. the SCI + vehicle group; $^{\&}P < 0.05$ vs. the SCI + NGR1 group. (e–g) Quantitative analysis of the mRNA expression of IL-6, IL-1β, and TNF-α in each group. $N = 3$. Data are represented as mean ± SEM. One-way analysis of ANOVA with Turkey's post hoc tests was used. $^{*}P < 0.05$ vs. the Sham + vehicle group; $^{\#}P < 0.05$ vs. the SCI + NGR1 group; $^{\&}P < 0.05$ vs. the SCI + NGR1 group. ANOVA, analysis of variance; HO-1, heme oxygenase-1; NGR1, notoginsenoside R1; Nrf2, nuclear factor erythroid 2 related factor 2; SCI, spinal cord injury.

of antiapoptotic proteins [40]. Our current result found a dramatic reinforcement of oxidant molecular MDA and a marked decline in the activities of antioxidant enzymes SOD and GSH-PX, which could be reserved by NGR1 administration after SCI. Interestingly, ML385 could partly inhibit the antioxidant effects of NGR1, which was consistent with the cardioprotective role of NGR1 treatment in myocardial ischemia/reperfusion [41]. In addition, previous study exhibits that NGR1 improved cardiac dysfunction via inhibiting the initiation of myocardia apoptosis [11]. Similarly, our Western Blot and TUNEL staining results found that SCI-induced reduction of Bcl-2 and enhancement of Cleaved caspase-9, Cleaved caspase-3, and Bax, and the percentage of TUNEL-positive neurons could also be improved by the administration of NGR1, whereas the suppression of Nrf2/HO-1 axis partly attenuated these antiapoptotic effects. What is more, HE staining and Nissl staining results showed that NGR1 treatment attenuated tissue damage and motor neuron loss in rats subjected to SCI. Taken together, these results suggested that the neuroprotective role of NGR1 administration through activating the Nrf2/HO-1 signaling pathway may be linked to the recovery of neuronal function after SCI.

Neuronal inflammation, triggered by SCI, is the main process of physiologic response leading to the activation of microglia, which further releases a great number of proinflammatory factors including TNF-α, IL-1 β, and IL-6 families (Carelli *et al*., 2015; Carelli *et al*., 2017). What is more, the over accumulation of spinal cord inflammatory cells due to the inflammatory cascade exacerbates the defects of neuronal function after SCI (Orr and Gensel, 2018). In addition, previous study shows that the upregulation of anti-inflammatory cytokine TSG-6 has been shown to exert its protective effects by promoting the axon regeneration and the formation of glial scar in the SCI model (Coulson-Thomas *et al*., 2016), which indicates the crucial role of anti-inflammation in the recovery of neuronal function. In our current study, we found an increase of proinflammatory cytokines TNF-α, IL-1 β, and IL-6, which indicated the progression of SCI. The treatment with NGR1 inhibited the upregulation of these proinflammatory cytokines, whereas the downregulation of Nrf2/HO-1 signaling pathway partly prevented the anti-inflammatory effects of NGR1, which was in line with previous finding evidences. This demonstrates that NGR1 administration

exhibited potent anti-inflammatory effect via PI3K/Akt axis in mice with cardiac dysfunction [11]. These findings showed that the activation of Nrf2/HO-1 signaling pathway is required for the attenuation of neuronal inflammation through NGR1 treatment.

Conclusion

In summary, our observations demonstrate that NGR1 administration may protect against SCI by inhibiting oxidative stress, neuronal apoptosis, and neuronal inflammation via activating the Nrf2/HO-1 signaling pathway. Our research provides a novel theoretical basis for NGR1 to improve the functional recovery of SCI rats.

Acknowledgements

This work was supported by the Startup Fund for scientific research from Fujian Medical University (grant number 2019QH1305).

H.L., Z.B., and M.Z. designed the study and completed the manuscript. H.L., Z.B., and Y.C. analyzed the data. Z.H. and H.L. interpreted the data and revised the language of the manuscript. Z.H. conceived the study. All authors read and approved the final manuscript.

Availability of data and materials: the datasets used during the current study are available from the corresponding author upon request.

Ethics approval and consent to participate: all study procedures were approved by the Ningde Municipal Hospital Institutional Animal Care and Use Committee and complied with the Guide for the Care and Use of Laboratory Animals.

Conflicts of interest

There are no conflicts of interest.

Reference

1 Ren H, Chen X, Tian M, Zhou J, Ouyang H, Zhang Z. Regulation of inflammatory cytokines for spinal cord injury repair through local delivery of therapeutic agents. *Adv Sci (Weinh)* 2018;**5**:1800529.
2 Orr MB, Gensel JC. Interactions of primary insult biomechanics and secondary cascades in spinal cord injury: implications for therapy. *Neural Regen Res* 2017;**12**:1618–1619.
3 Rios C, Santander I, Méndez-Armenta M, Nava-Ruiz C, Orozco-Suárez S, Islas M, *et al*. Metallothionein-I+II reduces oxidative damage and apoptosis after traumatic spinal cord injury in rats. *Oxid Med Cell Longev* 2018;**2018**:3265918.
4 Anwar MA, Al Shehabi TS, Eid AH. Inflammogenesis of secondary spinal cord injury. *Front Cell Neurosci* 2016;**10**:98.
5 Warden P, Bamber NI, Li H, Esposito A, Ahmad KA, Hsu CY, Xu XM. Delayed glial cell death following Wallerian degeneration in white matter tracts after spinal cord dorsal column cordotomy in adult rats. *Exp Neurol* 2001;**168**:213–224.
6 Bethea JR, Dietrich WD. Targeting the host inflammatory response in traumatic spinal cord injury. *Curr Opin Neurol* 2002;**15**:355–360.
7 Leung KS, Chan K, Bensoussan A, Munroe MJ. Application of atmospheric pressure chemical ionisation mass spectrometry in the identification and differentiation of Panax species. *Phytochem Anal* 2007;**18**:146–150.
8 Landgraeber S, Jäger M, Jacobs JJ, Hallab NJ. The pathology of orthopedic implant failure is mediated by innate immune system cytokines. *Mediators Inflamm* 2014;**2014**:185150.
9 Zhang HS, Wang SQ. Notoginsenoside R1 inhibits TNF-alpha-induced fibronectin production in smooth muscle cells via the ROS/ERK pathway. *Free Radic Biol Med* 2006;**40**:1664–1674.
10 Ning N, Dang X, Bai C, Zhang C, Wang K. Panax notoginsenoside produces neuroprotective effects in rat model of acute spinal cord ischemia-reperfusion injury. *J Ethnopharmacol* 2012;**139**:504–512.
11 Sun B, Xiao J, Sun XB, Wu Y. Notoginsenoside R1 attenuates cardiac dysfunction in endotoxemic mice: an insight into oestrogen receptor activation and PI3K/Akt signalling. *Br J Pharmacol* 2013;**168**:1758–1770.
12 Liu WJ, Tang HT, Jia YT, Ma B, Fu JF, Wang Y, *et al*. Notoginsenoside R1 attenuates renal ischemia-reperfusion injury in rats. *Shock* 2010;**34**:314–320.
13 Li Z, Li H, Zhao C, Lv C, Zhong CC, Xin W, *et al*. Protective effect of notoginsenoside R1 on an APP/PS1 mouse model of alzheimer's disease by up-regulating insulin degrading enzyme and inhibiting abeta accumulation. *CNS Neurol Disord Drug Targets* 2015; **14**: 360–369.
14 Sun Y, Liu T, Si Y, Cao B, Zhang Y, Zheng X, Feng W. Integrated metabolomics and 16S rRNA sequencing to investigate the regulation of Chinese yam on antibiotic-induced intestinal dysbiosis in rats. *Artif Cells Nanomed Biotechnol* 2019;**47**:3382–3390.
15 Andrews NC, Erdjument-Bromage H, Davidson MB, Tempst P, Orkin SH. Erythroid transcription factor NF-E2 is a haematopoietic-specific basic-leucine zipper protein. *Nature* 1993;**362**:722–728.
16 Loboda A, Damulewicz M, Pyza E, Jozkowicz A, Dulak J. Role of Nrf2/HO-1 system in development, oxidative stress response and diseases: an evolutionarily conserved mechanism. *Cell Mol Life Sci* 2016;**73**:3221–3247.
17 Bassermann F, Eichner R, Pagano M. The ubiquitin proteasome system - implications for cell cycle control and the targeted treatment of cancer. *Biochim Biophys Acta* 2014;**1843**:150–162.
18 Hirotsu Y, Katsuoka F, Funayama R, Nagashima T, Nishida Y, Nakayama K, *et al*. Nrf2-MafG heterodimers contribute globally to antioxidant and metabolic networks. *Nucleic Acids Res* 2012;**40**:10228–10239.
19 Wang X, Campos CR, Peart JC, Smith LK, Boni JL, Cannon RE, Miller DS. Nrf2 upregulates ATP binding cassette transporter expression and activity at the blood-brain and blood-spinal cord barriers. *J Neurosci* 2014;**34**:8585–8593.
20 Niture SK, Kaspar JW, Shen J, Jaiswal AK. Nrf2 signaling and cell survival. *Toxicol Appl Pharmacol* 2010;**244**:37–42.
21 Lin WP, Xiong GP, Lin Q, Chen XW, Zhang LQ, Shi JX, *et al*. Heme oxygenase-1 promotes neuron survival through down-regulation of neuronal NLRP1 expression after spinal cord injury. *J Neuroinflammation* 2016;**13**:52.
22 Lee SH, Kim Y, Rhew D, Kim A, Jo KR, Yoon Y, *et al* . Effect of canine mesenchymal stromal cells overexpressing heme oxygenase-1 in spinal cord injury. *J Vet Sci* 2017; **18**:377–386.
23 Lin Y, Vreman HJ, Wong RJ, Tjoa T, Yamauchi T, Noble-Haeusslein LJ. Heme oxygenase-1 stabilizes the blood-spinal cord barrier and limits oxidative stress and white matter damage in the acutely injured murine spinal cord. *J Cereb Blood Flow Metab* 2007;**27**:1010–1021.
24 Yacoub A, Hajec MC, Stanger R, Wan W, Young H, Mathern BE. Neuroprotective effects of perflurocarbon (oxycyte) after contusive spinal cord injury. *J Neurotrauma* 2014;**31**:256–267.
25 Li D, Tian H, Li X, *et al*. Zinc promotes functional recovery after spinal cord injury by activating Nrf2/HO-1 defense pathway and inhibiting inflammation of NLRP3 in nerve cells. *Life Sci* 2020:**117351**.
26 Mitsuhara T, Takeda M, Yamaguchi S, Manabe T, Matsumoto M, Kawahara Y, *et al*. Simulated microgravity facilitates cell migration and neuroprotection after bone marrow stromal cell transplantation in spinal cord injury. *Stem Cell Res Ther* 2013;**4**:35.
27 Jiang T, Yu JT, Zhu XC, Zhang QQ, Tan MS, Cao L, *et al*. Ischemic preconditioning provides neuroprotection by induction of AMP-activated protein kinase-dependent autophagy in a rat model of ischemic stroke. *Mol Neurobiol* 2015;**51**:220–229.
28 Dumont RJ, Verma S, Okonkwo DO, Hurlbert RJ, Boulos PT, Ellegala DB, Dumont AS. Acute spinal cord injury, part II: contemporary pharmacotherapy. *Clin Neuropharmacol* 2001;**24**:265–279.
29 Penas C, Guzmán MS, Verdú E, Forés J, Navarro X, Casas C. Spinal cord injury induces endoplasmic reticulum stress with different cell-type dependent response. *J Neurochem* 2007;**102**:1242–1255.
30 Tong Q, Zhu PC, Zhuang Z, Deng LH, Wang ZH, Zeng H, *et al*. Notoginsenoside R1 for organs ischemia/reperfusion injury: a preclinical systematic review. *Front Pharmacol* 2019;**10**:1204.
31 Zhou P, Xie W, Meng X, Zhai Y, Dong X, Zhang X, *et al* . Notoginsenoside R1 ameliorates diabetic retinopathy through PINK1-dependent activation of mitophagy. *Cells* 2019;**8**.

32 Zhang B, Zhang J, Zhang C, Zhang X, Ye J, Kuang S, *et al* . Notoginsenoside R1 protects against diabetic cardiomyopathy through activating estrogen receptor alpha and its downstream signaling. *Front Pharmacol* 2018; **9**:1227.

33 Chen PC, Vargas MR, Pani AK, Smeyne RJ, Johnson DA, Kan YW, Johnson JA. Nrf2-mediated neuroprotection in the MPTP mouse model of parkinson's disease: critical role for the astrocyte. *Proc Natl Acad Sci U S A* 2009;**106**:2933–2938.

34 Ramos-Gomez M, Kwak MK, Dolan PM, Itoh K, Yamamoto M, Talalay P, Kensler TW. Sensitivity to carcinogenesis is increased and chemoprotective efficacy of enzyme inducers is lost in nrf2 transcription factor-deficient mice. *Proc Natl Acad Sci U S A* 2001;**98**:3410–3415.

35 Wei W, Shurui C, Zipeng Z, Hongliang D, Hongyu W, Yuanlong L, *et al*. Aspirin suppresses neuronal apoptosis, reduces tissue inflammation, and restrains astrocyte activation by activating the Nrf2/HO-1 signaling pathway. *Neuroreport* 2018;**29**:524–531.

36 Huang Y, Li W, Su ZY, Kong AN. The complexity of the Nrf2 pathway: beyond the antioxidant response. *J Nutr Biochem* 2015;**26**:1401–1413.

37 Wang X, de Rivero Vaccari JP, Wang H, Diaz P, German R, Marcillo AE, Keane RW. Activation of the nuclear factor E2-related factor 2/antioxidant response element pathway is neuroprotective after spinal cord injury. *J Neurotrauma* 2012;**29**:936–945.

38 Liu NK, Xu XM. Neuroprotection and its molecular mechanism following spinal cord injury. *Neural Regen Res* 2012;**7**:2051–2062.

39 Zhang B, Bailey WM, McVicar AL, Gensel JC. Age increases reactive oxygen species production in macrophages and potentiates oxidative damage after spinal cord injury. *Neurobiol Aging* 2016;**47**:157–167.

40 Wang L, Li W, Kang Z, Liu Y, Deng X, Tao H, *et al*. Hyperbaric oxygen preconditioning attenuates early apoptosis after spinal cord ischemia in rats. *J Neurotrauma* 2009;**26**:55–66.

41 Yu Y, Fong PW, Wang S, Surya C. Fabrication of WS2/GaN p-n junction by wafer-scale WS2 thin film transfer. *Sci Rep* 2016;**6**:37833.